

Sol–Gel Synthesis of Organized Matter

Stephen Mann,* Sandra L. Burkett, Sean A. Davis, Christabel E. Fowler,
Neil H. Mendelson,[†] Stephen D. Sims, Dominic Walsh, and Nicola T. Whilton

School of Chemistry, University of Bath, Bath BA2 7AY, U.K., and Department of Molecular
and Cellular Biology, University of Arizona, Tucson, Arizona 85721

Received May 1, 1997. Revised Manuscript Received September 5, 1997[⊗]

In this review, we describe four approaches to the materials synthesis of organized inorganic matter. These include the use of self-assembled organic templates (transcriptive synthesis), cooperative assemblies of templates and building blocks (synergistic synthesis), spatially restricted reaction fields (morphosynthesis), and combinations of these approaches (integrative synthesis) in the area of sol–gel chemistry. We illustrate these strategies, respectively, by describing recent work on the formation of silica-based organized materials, viz. the preparation of ordered silica macrostructures using bacterial templates, template-directed synthesis of ordered hybrid mesophases and organoclays, synthesis of microskeletal frameworks of silica and other metal oxides in compartmentalized liquids, and use of bacterial superstructures in the fabrication of hierarchical macrostructures of mesoscopically ordered silica.

Introduction

It is becoming increasingly evident that complex inorganic materials can be synthesized across a range of length scales by constructional, morphological, and hierarchical coding of precipitation reactions.^{1,2} This new approach challenges the traditional view that inorganic solids are confined to the thermodynamic cul-de-sac of “condensed matter”. Instead, it offers a new paradigm of materials synthesis based on the notion of *organized-matter* chemistry. Implicit in this transformation is a shift in emphasis from the thermodynamic to kinetic regimes in which equilibrium phases are replaced by higher-order organizational states of consolidated matter. Achieving this goal requires new constructional mechanisms which generate structures that are determined by local rather than global energy minima. Moreover, the coordinated structuring of matter needs to be accomplished across a range of length scales if complex multicomponent materials are to be produced. All of this requires a chemistry far beyond the unit cell in which molecular-based processes are used to couple synthesis with construction.

Exploring this theme of “molecular tectonics”³ in biomineralization highlights the close relationship that exists between organized-matter chemistry and biology (Figure 1). Organisms use organic macromolecules and microstructures to control the nucleation and growth of inorganic minerals, and similar approaches are being developed in synthetic materials chemistry. So far, two main strategies are being explored. In the first, molecular or supramolecular templates are present as directing agents in the synthesis solution. These may take the form of discrete aggregates, such as dispersed micelles, or extended architectures, such as liquid crystalline mesophases. They can be self-assembled before or coassembled during synthesis and in both

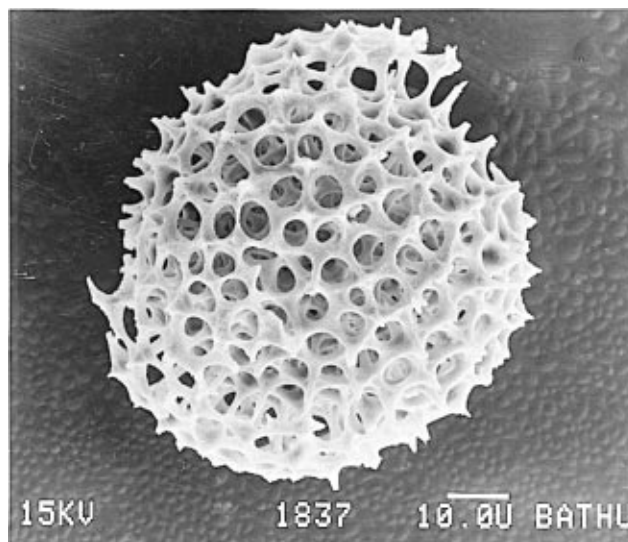


Figure 1. Scanning electron micrograph of a silica microskeleton formed by biomineralization in a single-celled organism. The image clearly illustrates the sophistication of biological processes in the synthesis of organized inorganic matter. Recent developments in inorganic materials chemistry suggest that structures with analogous complexity will become available by direct synthesis. Photograph, courtesy of John Forsdyke, University of Bath.

cases act as organized substrates for inorganic deposition. In the second approach, inorganic materials synthesis is spatially restricted by confining the reaction solutions within organized media. Typically, precipitation reactions are carried out in compartmentalized liquids such as micelles, vesicles, and microemulsions formed in mixtures of oil, water, and surfactant. In both approaches, the chemical, spatial, and structural properties of the template or enclosed reaction environment should complement the reaction chemistry, bonding, and packing considerations of the incipient inorganic phase. This requirement for interfacial matching is a major challenge in developing integrated inorganic–organic systems capable of coordinated assembly.

* Corresponding author. Tel: 44-1225-826122. Fax: 44-1225-826231.
E-mail: s.mann@bath.ac.uk.

[†] University of Arizona.

[⊗] Abstract published in *Advance ACS Abstracts*, November 1, 1997.

In this paper, we describe four approaches to organized-matter chemistry as applied to materials synthesis.² These are (i) *transcriptive synthesis*, which uses preorganized, self-assembled organic templates for materials structuring, (ii) *synergistic synthesis*, in which inorganic precursors and directing agents are coassembled into patterned architectures, (iii) *morphosynthesis*, which exploits chemical transformations in spatially restricted reaction fields to produce materials with complex form, and (iv) *integrative synthesis*, in which combinations of the above methods are used simultaneously to generate hierarchical materials. In each case, we illustrate the underlying principles by describing recent work on sol-gel routes to organized materials and composites. In particular, we discuss (a) the use of preorganized bacterial superstructures and silica nanoparticles in the formation of ordered silica macrostructures, (b) the direct synthesis of ordered covalently linked inorganic-organic hybrids, such as hexagonal organo-silica-surfactant mesophases and lamellar magnesium organosilicate clays, by template-directed cocondensation of tetraalkoxysilanes and functionalized organotrialkoxysilanes, (c) the use of phase partitioning accompanying the reaction $[\text{Si}(\text{OR})_4](\text{oil}) \rightarrow [\text{Si}(\text{OR})_{4-n}(\text{OH})_n](\text{aq})$ for the patterning of micrometer-scale silica frameworks in frozen-oil bicontinuous microemulsions, (d) the preparation of thin cellular films of transition metal oxides by redox/hydrolysis reactions in self-organized oil/water foams.

1. Transcriptive Synthesis

The formation of organized inorganic materials by direct templating using preformed self-assembled organic architectures can be described by the following sequence:

self-assembly \rightarrow transcription \rightarrow replication

In general, the organic template is in place prior to the formation of the inorganic phase and should be relatively stable throughout materials synthesis. To obtain inorganic replicas with high fidelity, interactions at the organic surface should be competitive over analogous processes in bulk solution. This is often accomplished by incorporating surface functional groups that direct interfacial events such as nucleation from supersaturated solutions and adsorption of incipient or preformed nanoclusters from colloidal sols. Templates with high specificity are in effect chemically coded surfaces that are transcribed at the molecular level into inorganic nuclei with precise structural, orientational, and positional properties. Repetition of these molecular processes in association with outgrowth along and within the template results in inorganic replication of the organic architecture. In this way, inorganic-organic hybrids with meso-, micro-, and macroscale patterns can be synthesized.

1.1. Supramolecular Templates and Chemical Reactivity. Many different organic molecules have been employed as directing agents for the control of pore shape and size in the synthesis of zeolites⁴ and nanoporous amorphous silicas.⁵ By comparison, there are few reports describing the use of preorganized organic templates for the sol-gel synthesis of materials exhibiting order on the meso- and microscopic length scales.

This is mainly because many of the possible candidate structures are disrupted under the chemical conditions employed. For example, the hydrolysis of tetraethyl orthosilicate (TEOS) produces numerous soluble silicate species, as well as ethanol and water (from further condensation), all of which can significantly perturb the phase behavior of organic aggregates such as vesicles and micelles. These interactions, nevertheless, are important aspects of the synergistic synthesis of MCM-41-type materials (section 2) and are responsible in part for morphosynthesis (section 3).

In a recent study, Tanev and Pinnavaia⁶ showed that porous pillared lamellar silicas could be prepared by confining the hydrolysis and condensation reactions of TEOS within the aqueous interlayer spaces of multilamellar vesicles preformed from the surfactant, 1,12-diaminododecane. The surfactant aggregates are sufficiently stable so that the mineralized replicas—in the form of spherical micrometer-size particles of concentrically arranged laminated silica-surfactant nanostructures—inherit the shape, size, and ultrastructure of the preformed self-assembled vesicles. These organized hybrids can be reduced to a mesoporous inorganic counterpart by removal of the template following solvent extraction and calcination.

In a related approach, an ordered liquid-crystalline hexagonal (H_1) mesophase of the nonionic surfactant, octaethylene glycol monohexadecyl ether, was used as an extended template for the formation of organized mesoporous silica.⁷ Although the production of methanol from tetramethyl orthosilicate (TMOS) hydrolysis temporarily destroys the H_1 phase, the high surfactant concentration (50 wt %) facilitates re-formation of the ordered structure in the presence of the incipient silicate species. Hydrolysis and condensation of TMOS are therefore spatially confined to the surface of the close packed rodlike micelles, with the result that a rigid monolith of the organized meso-structured material is produced by direct templating.

1.2. Biological Templates and Nanoparticle Building Blocks. In general, it seems reasonable that transcriptive mechanisms will lead to a direct correspondence in size and shape between template and inorganic replica. Thus, supramolecular assemblies will be of limited use for the chemical construction of micrometer-scale and macroscale structures. Increasing the length scale requires not only commensurate templates with higher-order architectures, but a move toward larger-scale building blocks. This is because the larger volume fraction of mineralized material is difficult to achieve from molecular precursors unless the system is under flow rather than batch conditions. Even then, infiltration of the template may be severely restricted by materials deposition in the near-surface regions of the organic architecture. One method of overcoming this problem is to use inorganic nanoparticles as preformed building blocks for the infiltration and mineralization of organized organic micro- and macroarchitectures.

In recent work, we used an organized bacterial superstructure consisting of coaligned multicellular filaments of *Bacillus subtilis* as our macroscale organic template⁸ (Figure 2). The bacterial superstructure, which is formed by slowly drawing a macroscopic thread from a web culture,⁹ resembles the arrangement of

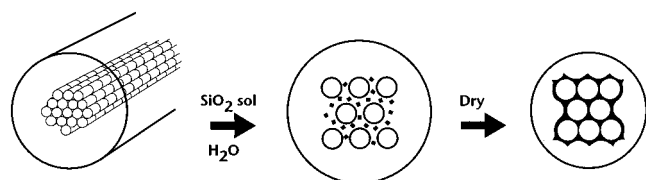


Figure 2. Formation of an organized macroporous silica framework using preorganized bacterial superstructural templates. On the left is a sketch of a dried macroscopic bacterial thread (ca. 0.2 mm in width) showing an ordered internal superstructure of 0.5 μm wide multicellular filaments. Infiltration and mineralization of the interfilament spaces of the thread (viewed in cross section) is achieved by reversible swelling in the presence of silica nanoparticles. Heating of the air-dried thread to 600 $^{\circ}\text{C}$ produces a macroporous replica.

surfactant cylinders in the H_I liquid-crystal phase, except, of course, that there is an increase in length scale of 2 orders of magnitude. In both cases, the interstitial spaces represent a continuum for patterned inorganic mineralization, but whereas the 1 nm wide contact spaces of the liquid-crystal array can be bridged by the in situ condensation of silicate anions (section 1.1), the formation of a coherent wall structure in the 100–200 nm wide interfilament spaces of the bacterial superstructure requires the use of a larger-scale constructional unit, viz. preformed silica nanoparticles.

Infiltration of the bacterial superstructure occurs as a direct consequence of the increase in volume associated with swelling of the thread when placed in aqueous solutions. Good penetration is achieved for silica colloids because the negative surface charge of the nanoparticles prevents aggregation with the highly anionic bacterial cell walls during infiltration. The particles therefore reside primarily in the interstitial void spaces of the superstructural template and thus can permeate deep into the bacterial thread. On drying, the thread

contracts and large increases in ionic strength occur within the interfilament regions. This has the effect of shielding the surface charge on the silica nanospheres such that a continuous mineral framework is formed by particle–particle aggregation (Figure 3). The thickness of the silica walls is ca. 200 nm in the void spaces, and 50 nm between the contact edges of adjacent filaments when sols with solid contents of 30 wt % are used. These bioinorganic materials can be heated to 600 $^{\circ}\text{C}$ to give ordered macroporous replicas which consist of parallel arrays of 0.5 μm wide channels aligned along the morphological axis of the intact fibrous product.

2. Synergistic Synthesis

Synergistic synthesis implies a mechanistic process in which cooperative interactions between different molecular components give rise to the chemical construction of organized states of matter. From an inorganic materials (sol–gel) perspective, this usually involves the interaction of inorganic precursors (silicate monomers, for example) and amphiphilic organic molecules in a three-step sequence:

coadaptation \rightarrow coassembly \rightarrow replication

The initial stage is characterized by structural and bonding complementarity at the inorganic–organic interface which result in coadaptation, rather than phase separation. For example, the synthesis of ordered mesoporous silica (MCM-41 and others¹⁰) is initiated by ion binding and exchange of soluble silicate species at the cationic headgroups of long chain quaternary ammonium salts present in weakly associated micellar microstructures.¹¹ The extent of coadaptation is very sensitive to the stoichiometry and relative chemical potentials of the reactants; that is, the balance of

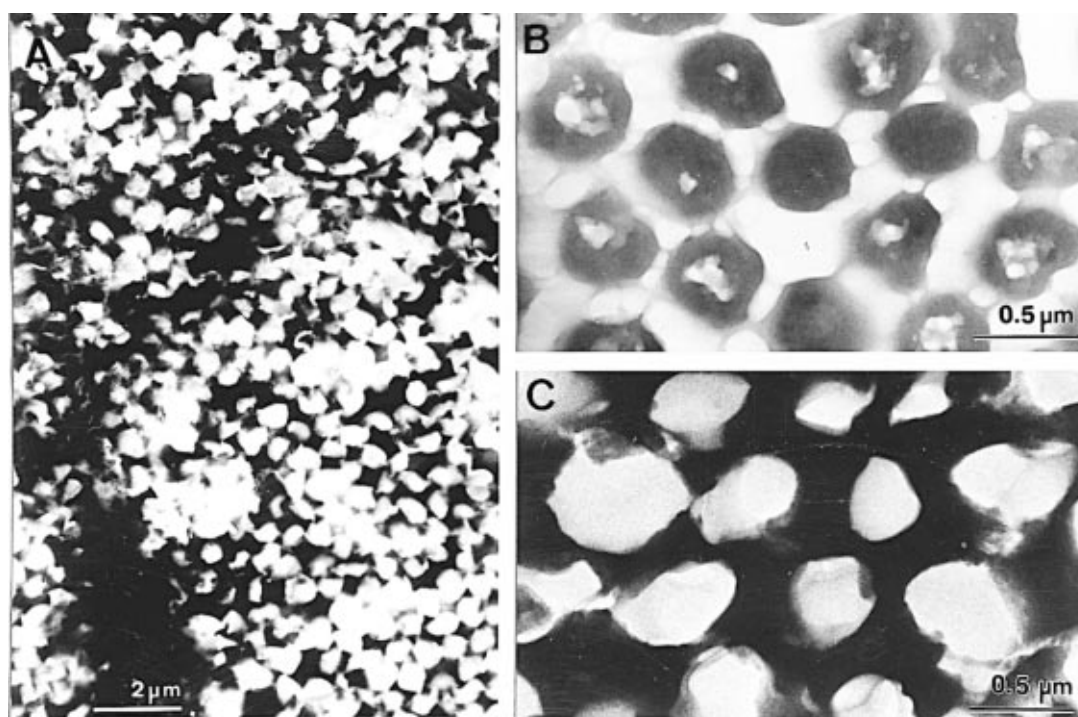


Figure 3. TEM images of sectioned bacterial thread viewed approximately parallel to the fiber axis: (a) low magnification image showing organized macroporous silica replica of the interfilament spaces; (b) high magnification image of unmineralized thread showing bacterial filaments and void spaces; (c) corresponding image of mineralized thread showing formation of continuous silica walls and encapsulated multicellular filaments.

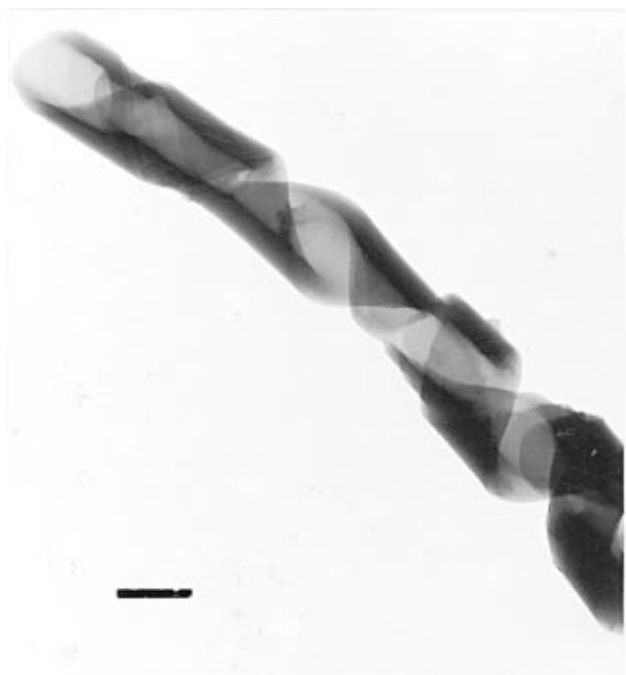


Figure 4. TEM image of a helical ribbon of a silica-phospholipid multilamellar biphasic. Scale bar = 500 nm.

thermodynamic and kinetic driving forces within the system. Under certain conditions, the interfacial energetics dominate and give rise to changes in the spatial charge density and steric requirements at the head-group-silicate interface. In the MCM-41 system, this generates a liquid crystalline hexagonal array of the surfactant-silicate salt that is coassembled by either *de novo* nucleation from ion pairs in solution or rearrangement and aggregation of coadapted micelles. Pattern replication then proceeds by further condensation and polymerization of silica within the interstitial spaces of the coassembled template. In many cases, postsynthesis removal of the organic phase affords an ordered mesoporous inorganic material with channel dimensions commensurate with the width of the rodlike surfactant micelles.

Recently we discovered that chiral lipid molecules and silicate anions could be assembled synergistically to produce a biphasic material with complex microscale morphology.¹² The structure was made using reaction conditions similar to those for the conventional room-temperature, acid-catalyzed synthesis of MCM-41, but with replacement of the surfactant by an unsaturated phospholipid, diacetylenic phosphatidylcholine. Unlike

previous work, in which this same phospholipid was used as a preformed template for the formation of hollow silica tubes,¹³ in our experiments, phospholipid crystallization and silica polymerization occur simultaneously. The result is a helical silica-lipid multilamellar microstructure (Figure 4). In the absence of TEOS, the phospholipid self-assembles into closed tubules, rather than the open ribbon structure of the biphasic, suggesting that coassembly leads to stabilization of the metastable form.

2.1. Ordered Organo-Silica-Surfactant Hybrid Mesophases. Considerable attention is now being focused on tailoring the chemical composition of ordered mesoporous silicas for possible applications. The introduction of inorganic heteroatoms (Al, Ti, V)¹⁴ into the silica framework, synthesis of non-silica analogues (oxides of Al, Ti, V, W, Sb, Pb),¹⁵ and attachment of metallocene derivatives via pendent Si-O-H groups (to form Si-O-metal linkages)¹⁶ have been explored as routes to the preparation of catalytically active, ordered mesophases. An additional route to functionalization that has been widely investigated in sol-gel silica chemistry¹⁷ involves the *cocondensation* of siloxane and organosiloxane precursors to produce inorganic-organic networks. In these materials, an organic moiety is covalently linked, via a nonhydrolyzable Si-C bond, to a siloxane species that is hydrolyzed to form a silica polymer. Because the formation of the silica walls in MCM-41 also occurs via siloxane hydrolysis and condensation, it seems feasible that cocondensation could be a viable approach to the synergistic synthesis of a wide range of organo-functionalized, covalently linked composites with ordered mesoporosity.

For this reason, we are currently investigating a range of systems involving cocondensation reactions and cooperative assembly for the synthesis of organized organo-silica-surfactant hybrid mesophases. A range of organically modified mesoporous silicas have been prepared at room temperature in the presence of surfactant ($C_{16}H_{33}N(CH_3)_3Br$, CTAB) micelles by the cocondensation of TEOS and organotrialkoxysilanes ($(R^*O)_3Si-R$, where $R = -C_6H_5$ (phenyltriethoxysilane, PTES), $-C_8H_{17}$ (octyltriethoxysilane, OTES) or $-CH_2-CHCH_2$ (allyltrimethoxysilane, ALTMS)¹⁸⁻²⁰ (Figure 5). A similar approach has been undertaken with TEOS and functionalized organotrialkoxysilanes, where $R = -(CH_2)_3SH$ ((3-mercaptopropyl)trimethoxysilane, TTMS), $-(CH_2)_3NH_2$ ((3-aminopropyl)triethoxysilane, ATES), $-(CH_2)_3OCH_2CH(O)CH_2$ ((3-(2,3-epoxypropoxy)propyl)trimethoxysilane, EPTMS), $-(CH_2)_3NCHNCH_2CH_2$ (3-

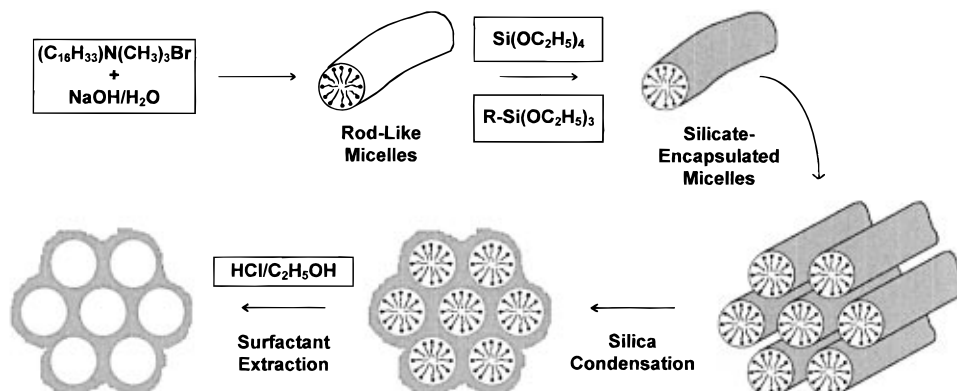


Figure 5. Scheme showing a generalized approach to the synergistic synthesis of an organized hybrid silica mesophase.

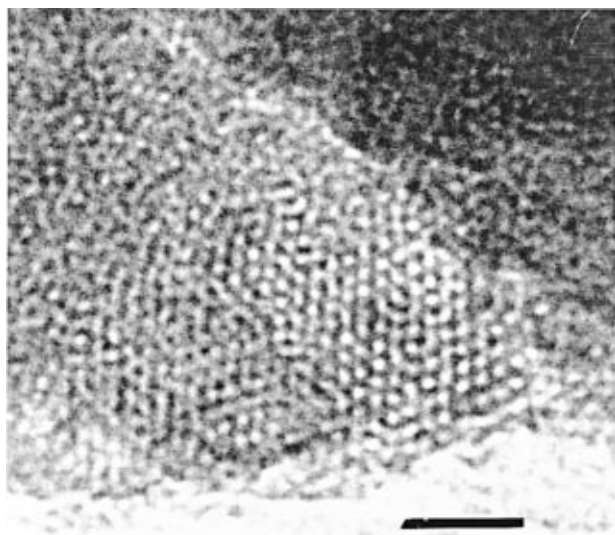


Figure 6. TEM micrograph of a hybrid mesoporous silica after surfactant extraction showing hexagonal order. The sample was prepared in the presence of 20 mol % phenyltriethoxysilane (PTES). Scale bar = 20 nm.

imidazolyltriethoxysilane, IMTES).²⁰ In general, covalently linked, hybrid mesoporous silicas with hexagonal order were synthesized using up to 20 mol % of the organosiloxane. In many cases, transmission electron microscopy (TEM) of the as-synthesized materials showed ordered hexagonal arrangements of lattice fringes. Similar images were also obtained for corresponding samples after removal of the surfactant template by solvent extraction (Figure 6). This was consistent with data obtained by small-angle X-ray diffraction (XRD), which showed higher-order hexagonal reflections for all the as-synthesized samples except the *n*-octyl-functionalized hybrid which was indexed as a disordered hexagonal phase. The unit cell parameters were dependent on the type of functionalization but, in general, were in the range 4–4.5 nm (as-synthesized).

²⁹Si MAS NMR spectroscopy of the as-synthesized materials has been used to determine quantitatively the extent of organosiloxane incorporation into the mesostructured silica materials. Distinct resonances were observed for the siloxane ($Q^n = \text{Si}(\text{OSi})_n(\text{OH})_{4-n}$, $n = 2-4$) and organosiloxane ($T^m = \text{RSi}(\text{OSi})_m(\text{OH})_{3-m}$, $m = 1-3$) units. Organosiloxane incorporation increased with increasing mole percent in the synthesis composition, although the relationship was not directly proportional, particularly for the functionalized organosiloxanes. Furthermore, for many of the materials, the relative amounts of ($Q^4 + T^3$), ($Q^3 + T^2$), and ($Q^2 + T^1$) species were essentially constant and equal to the respective Q^4 , Q^3 and Q^2 contents of the 100 mol % TEOS control sample. This observation suggests that the organosiloxane species are distributed uniformly throughout the silica network comprising the channel walls. Because the presence of some Q^4 centers is necessary to form the mesoporous architecture, there is likely to be an upper limit, <40 mol % on the basis of the Q^4 signal for the 100% TEOS-derived sample, to the extent of organosiloxane incorporation attainable in these ordered hybrid materials. Indeed, although the hexagonal order was usually preserved after surfactant extraction, lattice contractions were generally observed, suggesting that the presence of T^m centers significantly

increases the structural flexibility of the silica walls. This had the effect that some of the mesostructured materials, for example, the 20 mol % PTES hybrid, transformed into mesoporous phases with channel sizes around 2 nm.

These new results suggest that cocondensation of siloxane and organosiloxane precursors and their coassembly with surfactant templates should provide a general route to the synthesis of organically functionalized, uniformly porous, ordered silica materials with potential applications in organometallic chemistry, catalysis, and host-guest systems. A wide range of organosiloxane precursors could be used, although compounds that are very hydrophobic or for which the hydrolysis is slow relative to that of TEOS (the primary silica source) may become partitioned in the hydrophobic portion of the micelles rather than incorporated into the silica framework. In addition, some of the functionalized organosiloxanes were highly reactive—for example, ring-opening reactions were observed by ¹³C NMR for the epoxide derivatized silica-surfactant mesophases.

2.2. Organoclays. Although organic amphiphiles have significant advantages for the synergistic synthesis of organized matter—notably in establishing curvature and porosity—their limited use at moderate temperatures and in different solvents indicates that analogous inorganic-based templates could have significant advantages. One possibility that we are currently investigating is the direct synthesis of organo-functionalized claylike materials by hydrolysis of organotrialkoxysilanes in the presence of incipient magnesium hydroxide frameworks.²¹ As in the previous section, this is a strategy based on coassembly and cocondensation; in this system however, both the inorganic template and the silicate building blocks are generated by reaction with OH⁻ ions.

The structures of 2:1 trioctahedral phyllosilicate clays are constructed from inorganic lamellae, each of which comprises a sheet of octahedrally coordinated magnesium oxide/hydroxide chains (brucite sheets) overlaid on both sides with a tetrahedrally coordinated silicate layer. It has been proposed that the brucite sheets, which form by two-dimensional condensation, act as incipient templates for the subsequent condensation of the silicate layers.²² This seems feasible since there is a good epitaxial match at the brucite-silicate interface and appropriate chemical reactivity in the surface O/OH groups. We therefore investigated the possibility of coassembling brucite and organosilicate layers as an approach to the one-step synthesis of lamellar magnesium phyllo(organo)silicates containing ordered arrays of covalently linked organic functionalities.

It turns out that the procedure for making these organoclays is very straightforward. On the basis of a previous report,²³ organotrialkoxysilanes (methyltriethoxysilane ($R = \text{CH}_3$, MTES), PTES, or mixtures of MTES and PTES) and functionalized organotrialkoxysilanes ((3-ethylenediaminopropyl)trimethoxysilane (EDTMS), TTMS, ATEs, EPTMS, IMTES; see section 2.1 for details) were hydrolyzed at room temperature in basic methanolic solutions of magnesium chloride.^{21,24} The as-synthesized compounds were 2:1 trioctahedral phyllo(organo)silicates of approximate composition, $\text{Si}_8\text{R}_8\text{Mg}_6\text{O}_{16}(\text{OH})_4$ (based on the composition of the parent

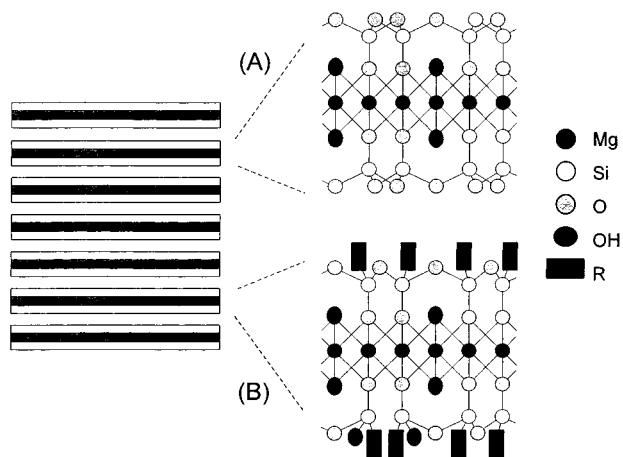


Figure 7. Schematic representation of the layered structures of (a) 2:1 trioctahedral phyllosilicate (talc) ($\text{Si}_8\text{Mg}_6\text{O}_{20}(\text{OH})_4$) and (b) magnesium organosilicates ($\text{Si}_8\text{R}_x\text{Mg}_6\text{O}_{16-x/2}(\text{OH})_{4+x}$; in this example, $x = 2$ to illustrate that not all of the organosiloxane centers are completely condensed).

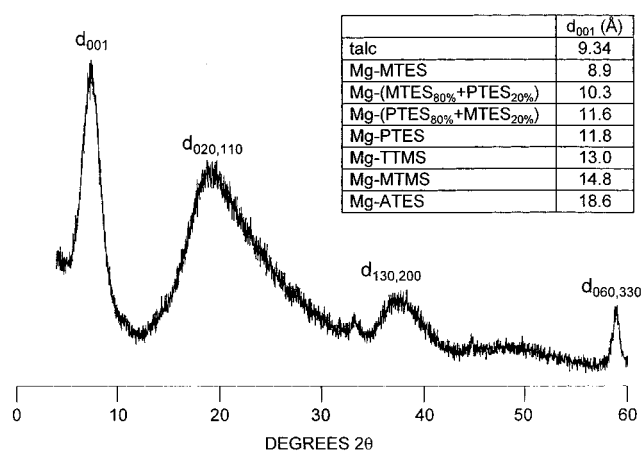


Figure 8. XRD pattern of Mg-PTES organoclay. Assignments are based on the 2:1 trioctahedral phyllosilicate structure of talc. Inset shows interlayer spacings for a range of organoclays synthesized. Note that the interlayer spacing indicated for talc is d_{002} , with two 2:1 trioctahedral phyllosilicate sheets per unit cell.

structure, talc, $\text{Si}_8\text{Mg}_6\text{O}_{20}(\text{OH})_4$). The materials were organized as lamellar inorganic-organic hybrids, with a constructional motif based on individual brucite sheets covalently linked on both sides to a layer of tetrahedral organosilicate units (Figure 7). The observed XRD reflections were broader than those from talc, suggesting significant intralayer disorder but the intralayer $d_{060,330}$ reflection (1.56–1.57 Å), which is characteristic of the 2:1 trioctahedral phyllosilicate structure, remained unchanged among the various magnesium organosilicates synthesized (Figure 8). Thus, the layered brucite framework can accommodate a range of pendent organic functionalities without the loss of long-range periodicity. Also, the interlayer d_{001} spacing increased with the steric size of the organosiloxane (Figure 8), but the absolute values were too small to be consistent with a regular bilayer motif.

Solid-state ^{29}Si NMR spectroscopy indicated that the silicon species were not fully condensed in the as-synthesized organoclays, possibly due to geometric packing constraints or to slow condensation kinetics or both. Silanol-containing T¹ and T² species were observed in addition to the fully condensed T³ centers.

Interestingly, no T³ species were present in the amino- and ethylenediaminopropyl phyllosilicates, and the T¹ signal was dominant in the imidazole-containing clay. This may reflect the disfavored condensation chemistry of hydrolyzed ATES²⁵ and related amino-functionalized organosiloxanes. The infrared spectrum of the ATES- phyllosilicate indicated that the amine groups were protonated and suggested the presence of an intercalated chloride counterion. This was consistent with the observation that the 3-aminopropyl-functionalized organoclay had a significantly larger interlayer spacing compared with that for the corresponding 3-mercapto- propyl phyllosilicate (Figure 8).

The limited coordination of the organosiloxane units, hydrophobicity of the organic moieties, and amphiphilic nature of the brucite-organosiloxane unit appear to facilitate formation of the lamellar architecture. Layered magnesium silicate structures do not form at room temperature in the absence of hydrophobic organosiloxane precursors, such as when triethoxysilane (HTES; R = H) or tetraethoxysilane (TEOS; R = OCH_2CH_3) is used in lieu of the organotrialkoxysilane component in the synthesis.

Organoclays prepared from functionalized organotrialkoxysilanes were shown by ^{13}C NMR spectroscopy to contain intact organic moieties. For example, no ring-opening reactions of the epoxy derivative occurred during clay synthesis. Thus, the procedure offers general scope for preparing organized arrays of reactive organic functionalities within an inorganic matrix. Several areas are currently under investigation.^{21,24} For example, thiol-containing clays can be oxidized to disulfides via treatment with aqueous hydrogen peroxide. Similarly, reaction of covalently linked phenyl groups with $\text{Mo}(\text{CH}_3\text{CN})_3(\text{CO})_3$ to form molybdenum arene carbonyl complexes was apparent by IR spectroscopy. The mercaptopropyl functionality was used to synthesize 2 nm size gold particles within the layers of the phyllo(organo)silicate via in situ reduction of tetrachloroauric(III) acid. However, the d_{001} reflection of the clay was no longer observed upon deposition of the gold nanoparticles, suggesting concomitant exfoliation or extensive expansion of the inorganic-organic lamellae.

3. Morphosynthesis

Chemists often focus on periodic order and thus tend to neglect the richness and importance of external morphological form, even though soft matter and the natural world are replete in complex systems exhibiting aperiodicity, curvature, hierarchy, and morphogenesis. These features are connected with patterning processes that arise from dynamic interactions and information transfer present within multicomponent systems.

How might inorganic materials with complex external forms be chemically synthesized? In previous sections of this review we have discussed how preorganized or coorganized templates can be used in the preparation of organized matter with dimensional, structural, and architectural specificity. In general, these template-directed approaches give rise to internalized organization within conventional forms such as powders, fibers, and thin films. We now describe an alternative approach—termed “morphosynthesis”^{3,26}—in which organized and delineated chemical environments—“reaction fields”—are employed in the in situ pattern generation

of inorganic-based materials with unusual and complex external morphologies.

3.1. Static Reaction Fields. The use of multiphase systems containing restricted aqueous/hydrophilic reaction environments has traditionally been concerned with the preparation of size-quantized dispersed inorganic nanoparticles. In this approach, the reaction field is delineated by the imposition of an external spatial boundary which is not significantly perturbed by the chemical processes. For example, reverse micelles and microemulsions have been used to prepare many different types of nanoparticles,^{27–29} including zeolites.³⁰ Similarly, nanocolloids with magnetic and semiconducting properties have been prepared in lipid vesicles^{31,32} as well as in the polypeptide micelle of the iron storage protein, ferritin.^{33,34} Recently, block copolymer micelles, consisting of hydrophobic and hydrophilic domains, have been used to produce ordered arrays of gold nanoparticles.³⁵

Clearly, this strategy could be extended to the synthesis of inorganic materials exhibiting complicated three-dimensional morphologies if analogous complex reaction fields can be prepared. One possible approach uses stabilized foams for the construction of inorganic materials with honeycomb morphologies.^{36–38} For example, foams of Freon (fluorotrichloromethane) droplets can be dispersed in water in the presence of a surfactant (sodium dodecyl sulfate) and cosurfactant (1-dodecanol). Addition of an alkaline silica sol and adjustment to acidic pH values results in the in situ gelation of the foam structure and the formation of a cellular inorganic architecture.³⁶ Ceramic foams of mullite ($3\text{Al}_2\text{O}_3 \cdot 2\text{SiO}_2$) were also prepared in a similar procedure using a mixture of silica and boehmite (AlOOH) colloidal sols.³⁶ The sintered materials retained the cellular architecture, with cell sizes ranging from 30 to 1000 μm .

3.2. Reconstructive Reaction Fields. In recent work, we have investigated the use of bicontinuous microemulsions, assembled from mixtures of tetra- and hexadecane, water, and the cationic surfactant didodecyltrimethylammonium bromide (DDAB), in inorganic materials synthesis. These microemulsions are structured as compartmentalized liquids in which the oil and water components are separated into highly branched and interconnected nanoscale networks. By using a supersaturated aqueous phase in place of water and freezing the oil channels at temperatures above 0 °C, our aim was to transcribe the complex morphology of the assembled reaction field into a nanotextured inorganic replica. To our surprise, studies of calcium phosphate precipitation in bicontinuous microemulsions^{39,40} produced materials with remarkable interconnected architectures on length scales 2 orders of magnitude greater than that of the compartmentalized reaction environment. Although nucleation and initial growth of the inorganic phase appeared to replicate the arrangement of the nanoscale water conduits, later stages of growth were accompanied by reconstruction of localized regions of the microemulsion structure. The latter process seems to develop from interactive coupling of the crystallization process and surrounding reaction environment. This is a time-dependent process such that morphological patterns at the micrometer scale evolve from the nanoscale replica through a series of intermediate structures facilitated by the reconstructive

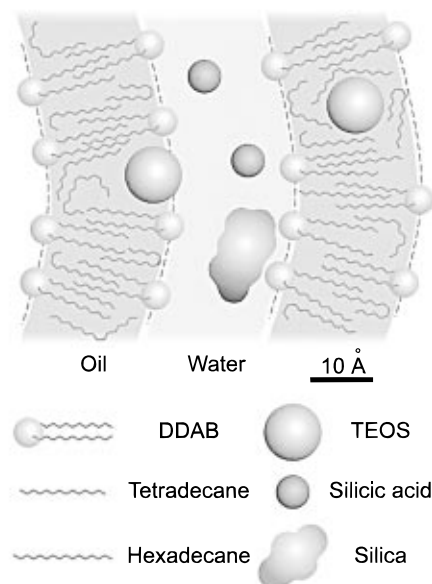


Figure 9. Sketch of a bicontinuous microemulsion showing 2 nm oil and water channels stabilized by the surfactant DDAB. Precipitation of silica specifically within the water channels occurs by slow hydrolysis of TEOS partitioned in the oil phase. The oil matrix is frozen to increase the rigidity of the system.

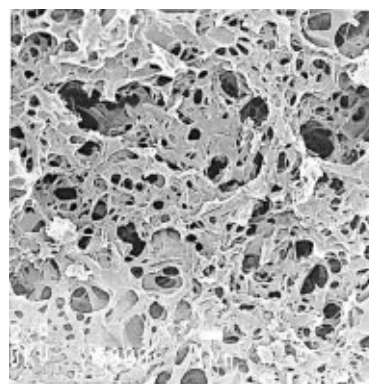


Figure 10. Scanning electron microscopy (SEM) micrograph of an interconnected macroporous framework of amorphous silica synthesized in a bicontinuous microemulsion. Scale bar = 1 μm .

tional properties of the organized media. Overall, the synthesis can be described as

reaction assembly \rightarrow replication \rightarrow metamorphism

Work currently in progress has shown that sol-gel processes can be integrated into this approach to inorganic morphosynthesis. Unlike the calcium phosphate materials which were deposited directly from the supersaturated aqueous channels of the bicontinuous microemulsions, interconnected frameworks of silica were synthesized from TEOS solubilized in the oil conduits.⁴¹ Reaction of TEOS at the oil-surfactant-water interface results in phase partitioning as the hydrolysis products are water soluble. This, together with freezing the oil prior to reaction, gives rise to the controlled precipitation of silica in the nanoscopic water channels (Figure 9). If left for several days however, extended three-dimensional open frameworks of amorphous silica are produced (Figure 10). The microstructures, which consist of thin interconnected mineral sheets, remain intact after calcining at 600 °C. Similar

experiments with frozen reverse micelles gave networks of micrometer-sized spherical particles.⁴¹

The results indicate that the composition, viscosity, and structure of the microemulsions have a profound influence on the general morphological features of the associated silica phase, but that the fidelity of this pattern replication is low because, although there is morphological correspondence, the length scales of the reaction media and inorganic products are very different. Significantly, small-angle X-ray scattering studies of silica polymerization in DDAB microemulsions⁴² indicate that the nanoscopic bicontinuous structure is retained between modified regions, presumably containing the larger-scale microstructures of the deposited materials. Thus, progressive polymerization of the silica phase has a localized effect, but most of the bicontinuous microstructure remains intact. One major factor likely to influence the local phase structure is the production of ethanol from the hydrolysis/condensation reactions. Other possible mechanisms include surface hydration of the inorganic material, surface adsorption of surfactant, and disruption of the oil matrix by TEOS phase transfer. The overall effect is that the silica network "evolves" by coupling of these processes with ongoing polymerization such that morphological patterns on the micrometer scale develop by the interactive reconstruction of the reaction field.

3.3. Transitory Reaction Fields. A further approach to inorganic morphosynthesis involves the materials replication of transitory reaction fields. To this end, the induction of microphase separation in self-organized media can give rise to transient metastable structures, such as foams and vesicle aggregates, which can be used to generate boundary surfaces and imprints for the in situ sculpturing of inorganic materials. An important aspect of this strategy lies in establishing a sequence of steps, viz.

reaction assembly → transformation → replication

in which the onset of inorganic precipitation and formation of the transitional structure must be synchronized if the inorganic patterns are to be replicated prior to disintegration of the self-organized reaction field. Although this is often difficult to achieve without recourse to empirical studies, the involvement of unstable organizational states does offer the possibility of synthesizing highly unusual inorganic morphologies and architectures.

This approach has been used to prepare honeycomb frameworks of either mesoporous or macroporous calcium carbonate (aragonite) by solvent extraction of supersaturated microemulsions spread onto metal substrates.⁴³ Hollow shells of the cellular calcium carbonate architecture were also fabricated by applying this method to micrometer-size polystyrene beads coated in the supersaturated microemulsion.⁴³ The cellular architecture originates from rapid mineralization around a biliquid foam of self-organized oil droplets which form in the microemulsion thin film by demixing during solvent extraction. Because the foam is a transitory structure, mineralization and oil droplet self-assembly must occur almost simultaneously if the interstitial spaces are to be filled with a continuous inorganic framework. This is achieved by outgassing of CO₂ from the supersaturated solution, which, although negligible

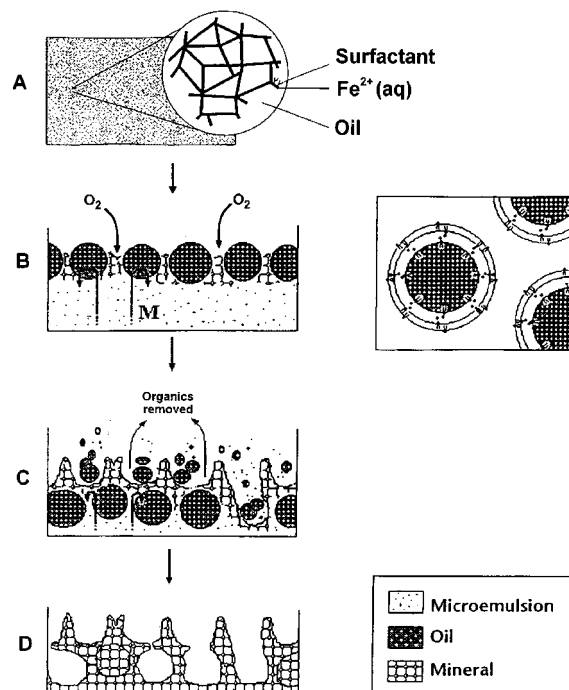


Figure 11. Proposed mechanism of formation of thin cellular frameworks of transition metal oxides. (A) Bicontinuous microemulsion containing deaerated metal ion solution (eg. Fe(II) or Mn(II)). (B) Washing in hot chloroform results in self-organization of mesoscopic oil droplets by Marangoni convection (M), and metal ion oxidation at the extended air-water interface. Hydrolysis of the oxidized species results in metal oxide deposition within the continuous aqueous layer surrounding the oil droplets. Inset shows a top view of the proposed arrangement, with the oil droplets stabilized by a thin soapy aqueous film which is distinct from the continuous phase of the metal ion containing solution. (C) Continued washing removes oil and surfactant, leaving the mineralized boundary walls and a second layer of organized oil droplets. (D) Complete removal of the oil and surfactant result in a mineralized replica of the foaml like reaction media.

in the bulk microemulsion, becomes rapidly accelerated as the air-water interface increases in area during foam formation.

In current work⁴⁴ we have shown that cellular films of transition metal oxides can be fabricated by similar processes involving rapid increases in metal-ion oxidation associated with the formation of the extended air-water interface of the biliquid foam (Figure 11). The enhanced rate of oxidation is accompanied by patterned sol-gel reactions within the interstitial spaces of the incipient foam. For example, hot hexane dip-washing of a thin layer of a DDAB/C₁₄H₃₀ bicontinuous microemulsion containing either degassed Fe(II) or Mn(II) solution produced cellular films of crystalline iron(III) oxide or manganese(III/IV) oxide, respectively (Figure 12). The mineral walls were continuous, branched, and approximately 50 nm (FeOOH) or 100 nm (Mn oxide) in width and enclosed cells of average size, 100 or 300 nm, respectively. The complex morphology was only established if the rates of aerial oxidation and hydrolytic condensation were commensurate with the lifetime of the biliquid foam. In this regard, the ease with which transition metals can be oxidized at the air-water interface is of key importance. Thus, whereas substrates could be readily coated with a cellular film of FeOOH at pH 3.8, the formation of a Mn(III/IV) oxide honeycomb architecture required a higher pH of 7.6. The

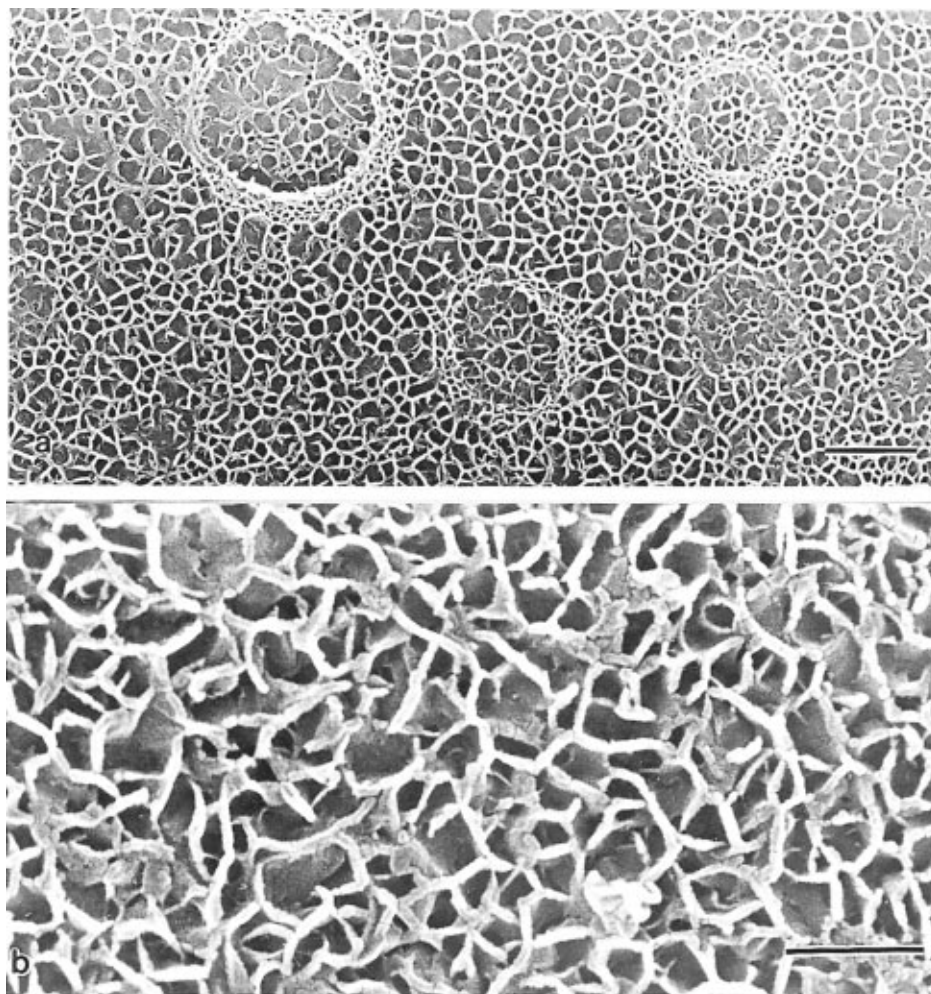


Figure 12. SEM micrographs of cellular transition metal oxide thin films of (a) Mn(III/IV) oxide with additional micrometer-scale morphological features superimposed on the cellular framework, scale bar = $2\ \mu\text{m}$; (b) iron(III) oxide, (lepidocrocite, FeOOH) showing mineralized walls and disordered junctions, scale bar = $0.5\ \mu\text{m}$.

reduced rate of Mn(II) oxidation, compared with that of Fe(II), produces a mixed valence nonstoichiometric oxide rather than a pure MnO_2 phase. Moreover, these kinetic constraints could also be responsible for larger morphological structures superimposed on these cellular films (Figure 12a) because the microphase separation and demixing processes are more advanced prior to mineral deposition in the boundary spaces. This leads to a greater variation in the reorganizing microstructures and the coalescence of oil droplets into larger oil spheres, which are then replicated in the mineral pattern.

Although the cellular films were polycrystalline at the macroscopic level, the mineralized walls and associated junctions were shown by TEM studies to be constructed from units that are continuous single crystals on the length scale of hundreds of nanometers.⁴⁴ This suggests that in each system the connectivity in the wall structure is established from multiple nucleation centers which develop as single crystals until they encounter neighboring outgrowths.

In principle it should be possible to induce a series of localized phase separations on different length scales so that a hierarchy of inorganic patterns can be replicated. Sol-gel chemistry could be an important component in realizing this objective. For example, heat treatment of hydrated aluminum hydroxyoxide with a decylammonium dihydrogenphosphate lamellar precu-

ror in tetraethylene glycol produced mesolamellar aluminophosphate with complex, hierarchical form. A range of microscopic pores and surface patterns were imprinted on macroscopic architectures such as solid spheroids and hollow shells.^{45,46} These features appear to be generated by the adhesion of mesolamellar aluminophosphate vesicles with higher-order vesicular aggregates formed by microscopic phase separation, fusion, and reshaping.

4. Integrative Synthesis

Several approaches to the sol-gel derived synthesis of organized materials have been described in this review. In this final section we discuss the possibility of combining these strategies to prepare materials with hierarchical structure and morphology.

The work to date has focused on the development of systems which contain templates/directing agents expressed simultaneously on at least two different length scales. This has involved coupling the synergistic synthesis of silica-surfactant mesophases with higher-order transcriptive patterning. For example, undertaking the synthesis in an oil/water emulsion produces hollow macroscopic spheres of mesoporous silica.⁴⁷ A hierarchical material is formed as a consequence of the coassembly of surfactant and silica at the surface of dispersed oil droplets, several micrometers in diameter.

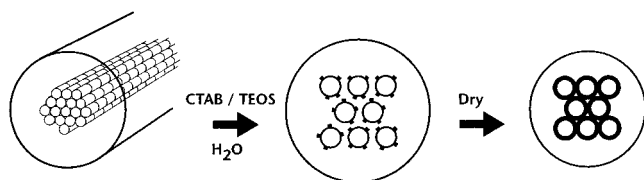


Figure 13. Formation of a hierarchical silica-based structure. A dried macroscopic bacterial thread (sketch on left), consisting of an ordered superstructure of $0.5 \mu\text{m}$ wide multicellular filaments, is infiltrated and mineralized within the interfilament spaces with the silica-surfactant mesophase, MCM-41. This is achieved by dipping the thread into an alkaline synthesis mixture (CTAB/TEOS) and air-drying. MCM-41 particles are closely associated with the cell walls of the bacterial filaments. Controlled heating removes the organic material to produce a macroporous replica consisting of micrometer-size channels with walls of mesoporous silica.

The oil droplets contain TEOS and surfactant molecules. The former is hydrolyzed and the latter enriched at the oil-water interface, such that the emulsion droplets act as macroscopic templates for the nucleation of the silica-surfactant biphasic.

Another recent report has illustrated how supramolecular and supercellular templates can be combined for the fabrication of inorganic materials with structural hierarchy.⁸ Again, the approach integrates two synthesis strategies. In this case, however, the coassembly of a silica-surfactant mesophase is patterned within a biological superstructure consisting of coaligned multicellular filaments of *Bacillus subtilis*, (Figure 13). Dried bacterial thread was dipped into an alkaline synthesis solution, 3 min after mixing together the surfactant (CTAB) and TEOS, and withdrawn after 60 min. The air-dried product was extensively mineralized throughout the thread such that the multicellular filaments were encased in an extended polycrystalline framework of the silica-surfactant mesophase. The mesostructured interfilament walls were often thinner (ca. 100 nm) and less ordered than those for the pure silica frameworks (section 1.2) but remained intact after the bacteria and surfactant were removed by heating to 600

°C. The resulting intact fiber consists of a macroporous framework of coaligned $0.5 \mu\text{m}$ wide channels enclosed in walls of mesoporous silica. Fractured samples show the presence of discrete hollow cylinders of mesoporous silica (Figure 14), suggesting that the organized composite is assembled by templating the mesophase on the surface of the bacterial filaments and not, as in the case of the pure silica material (see section 1.2), from the consolidation of weakly associated nanoparticles within the interfilament spaces.

These initial investigations suggest that other biological superstructures with reversible swelling properties should have potential uses as templates for the micrometer-scale assembly of ordered porous ceramic architectures. Synthetic polymer fibers and structured organic composites could also be exploited. The immediate challenge is to discover hosts that remain essentially unperturbed when infiltrated by synthesis solutions and which in turn do not significantly influence the reaction chemistry of the guest species.

Concluding Remarks

The imposition of structural and morphological patterns at a scale larger than the molecular necessitates the use of intrinsic and extrinsic directing agents in inorganic materials synthesis. This review has described some recent developments which illustrate that ordered materials can be formed by incorporating organizational processes into sol-gel chemistry. The motivation for chemically constructing these materials reflects a general shift in academic focus toward the notion of complexity as well as the awareness that new speciality products are being demanded in many applications. While it is difficult to predict the future, inorganic materials with multilevel structures and architectures are likely to find uses in determining catalytic activity, flow and transport behavior, separation efficiency, acoustic regulation, storage, delivery and release rates, and biocompatibility.

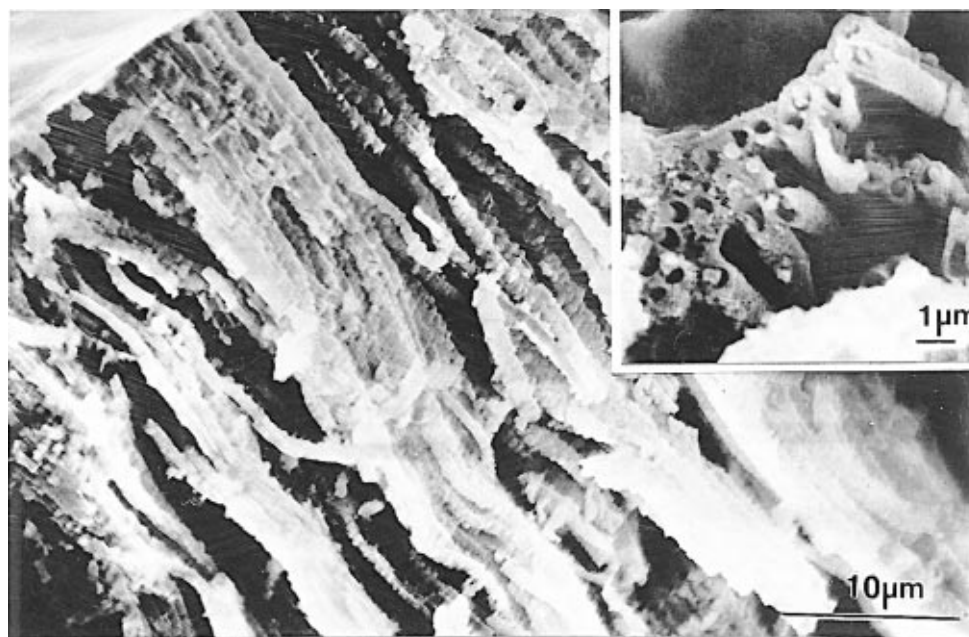


Figure 14. SEM image of MCM-41 infiltrated bacterial thread after heating to 600 °C and fractured parallel to the fiber axis, showing intact hollow cylinders of mesoporous silica. Inset: transverse view of calcined thread showing hollow MCM-41 tubules.

Acknowledgment. The authors acknowledge financial support from the Engineering and Physical Sciences Research Council, Biotechnology and Biological Sciences Research Council, The Wellcome Trust, BNFL plc, English China Clays International, and the University of Bath. We thank Dr. D. C. Apperley at the University of Durham for solid-state NMR spectroscopy.

References

- (1) Mann, S. *J. Mater. Chem.* **1995**, *5*, 935.
- (2) Mann, S.; Ozin, G. A. *Nature* **1996**, *382*, 313.
- (3) Mann, S. *Nature* **1993**, *365*, 499.
- (4) Zones, S. I.; Davis, M. E. *Curr. Opin. Solid State Mater. Sci.* **1996**, *1*, 107.
- (5) Raman, N. K.; Anderson, M. T.; Brinker, C. J. *Chem. Mater.* **1996**, *8*, 1682.
- (6) Tanev, P. T.; Pinnavaia, T. J. *Science* **1996**, *271*, 1267.
- (7) Attard, G. S.; Glyde, J. C.; Goltner, C. G. *Nature* **1995**, *378*, 366.
- (8) Davis S. A.; Burkett, S. L.; Mendelson, N. H.; Mann, S. *Nature* **1997**, *385*, 420.
- (9) Mendelson, N. H. *Proc. Natl. Acad. Sci. U.S.A.* **1978**, *75*, 2478.
- (10) Kresge, C. T.; Leonowicz, M. E.; Roth, W. J.; Vartuli, J. C.; Beck, J. S. *Nature* **1992**, *359*, 710.
- (11) Firouzi, A.; et al. *Science* **1995**, *267*, 1138.
- (12) Burkett, S. L.; Mann, S. Unpublished data.
- (13) Baral, S.; Schoen, P. *Chem. Mater.* **1993**, *5*, 145.
- (14) Huo, Q.; et al. *Chem. Mater.* **1994**, *6*, 1176.
- (15) Antonelli, D. M.; Ying, J. Y. *Angew. Chem., Int. Ed. Engl.* **1995**, *34*, 2014.
- (16) Maschmeyer, T.; Rey, F.; Sankar, G.; Thomas, J. M. *Nature* **1995**, *378*, 159.
- (17) Sanchez, C.; Ribot, F. *New J. Chem.* **1994**, *18*, 1007.
- (18) Burkett, S. L.; Sims, S. D.; Mann, S. *Chem. Commun.* **1996**, 1367.
- (19) Sims, S. D.; Burkett, S. L.; Mann, S. *Proc. Spring Meet. Mater. Res. Soc.* **1996**, *431*, 77.
- (20) Fowler, C. E.; Burkett, S. L.; Mann, S. *Chem. Commun.* **1997**, 1769.
- (21) Burkett, S. L.; Press, A.; Mann, S. *Chem. Mater.* **1997**, *9*, 1071.
- (22) Carrado, K. A. *Ind. Eng. Chem. Res.* **1992**, *31*, 1654.
- (23) Fukushima, Y.; Tani, M. *Chem. Commun.* **1995**, 241.
- (24) Whilton, N. T.; Burkett, S. L.; Mann, S. Unpublished data.
- (25) Ishida, H.; Chiang, C. H.; Koenig, J. L. *Polymer* **1982**, *23*, 251.
- (26) Ozin, G. A. *Acc. Chem. Res.* **1997**, *30*, 17.
- (27) Pileni, M. P.; Motte, L.; Petit, C. *Chem. Mater.* **1992**, *4*, 338.
- (28) Roman, J. P.; Hoornaert, P.; Faure, D.; Biver, C.; Jacquet, F.; Martin, J. M. *J. Colloid Interface Sci.* **1990**, *144*, 324.
- (29) Arriagada, F. J.; Osseo-Asare, K.; *J. Colloid Interface Sci.* **1995**, *170*, 8.
- (30) Jakupca, M.; Reddy, S. N.; Salvati, L.; Dutta, P. K. *Nature* **1995**, *374*, 44.
- (31) Mann, S.; Hannington, J. P.; Williams, R. J. P. *Nature* **1986**, *324*, 565.
- (32) Bhandarkar, S.; Bose, A. *J. Colloid Interface Sci.* **1990**, *135*, 531.
- (33) Meldrum, F. C.; Heywood, B. R.; Mann, S. *Science* **1992**, *257*, 522.
- (34) Wong, K. K. W.; Mann S. *Adv. Mater.* **1996**, *8*, 928.
- (35) Spatz, J. P.; Roescher, A.; Möller, M. *Adv. Mater.* **1996**, *8*, 337.
- (36) Wu, M.; Fujii, T.; Messing, G. L. *J. Non-Cryst. Sol.* **1990**, *121*, 407.
- (37) Morgan, J. S.; Wood, J. L.; Bradt, R. C. *Mater. Sci. Eng.* **1981**, *47*, 37.
- (38) Lange, F. F.; Miller, K. T. *Adv. Ceram. Mater.* **1987**, *2*, 827.
- (39) Walsh, D.; Hopwood, J. D.; Mann, S. *Science* **1994**, *264*, 1576.
- (40) Walsh, D.; Mann, S. *Chem. Mater.* **1996**, *8*, 1944.
- (41) Sims, S. D.; Walsh, D.; Mann, S. *Adv. Mater.*, in press.
- (42) Burban, J. H.; He, M.; Cussler, E. L. *AIChE J.* **1995**, *41*, 159.
- (43) Walsh, D.; Mann, S. *Nature* **1995**, *377*, 320.
- (44) Walsh, D.; Mann, S. *Adv. Mater.* **1997**, *9*, 658.
- (45) Oliver, S.; Kuperman, A.; Coombs, N.; Lough, A.; Ozin, G. A. *Nature* **1995**, *378*, 47.
- (46) Ozin, G. A.; Oliver, S. *Adv. Mater.* **1995**, *7*, 943.
- (47) Schacht, S.; Huo, Q.; Voight-Martin, I. G.; Stucky, G. D.; Schüth, F. *Science* **1996**, *273*, 768.

CM970274U